Differential Geometric Modelling and Robust Path Following Control of Snake Robots Using Sliding Mode Techniques

Ehsan Rezapour, Kristin Y. Pettersen, Pål Liljebäck, and Jan T. Gravdahl

***Abstract*— This paper considers straight line path following control of wheel-less planar snake robots using sliding mode techniques. We first derive the Poincaré representation of the equations of motion of the robot using the techniques of differential geometry. Furthermore, we use partial feedback linearization to linearize the directly actuated part of the system dynamics. Subsequently, we propose an analytical solution to the robust path following control problem in two steps. In the first step, we use sliding mode techniques to design a robust tracking controller for the joints of the robot to track a desired gait pattern. In the second step, we stabilize an appropriately defined sliding manifold for the underactuated configuration variables of the robot, thereby guaranteeing convergence of the robot to the desired straight path. The paper presents simulation results which validate the theoretical results.**

I. INTRODUCTION

Wheels and legs have been the primary locomotion tools for biologically inspired robots on flat surfaces. However, challenging environments where the surfaces are irregular and unstructured, may significantly degrade the performance of such robots. Under these circumstances, snake robots are an interesting alternative to wheel and leg based robots due to their long and slender body. The many degrees-of-freedom (DOF) of snake robots provide adaptability properties and enable them to maintain mechanical stability even during failure of some of their actuators. Motion control of snake robots is, however, challenging due to the underactuation, which is characterized by fewer independent control inputs than DOF, complex gait patterns, and complicated force interactions with their environments. Mine detection and elimination, firefighting operations, and industrial operations in narrow environments are typical areas where the structural flexibility properties of snake robots have made them an interesting choice for applications.

This paper considers path following control of snake robots. Path following involves making the outputs of the motion control system converge to and follow a desired planar path while guaranteeing forward motion along the path and boundedness of the system states. This problem is particularly relevant for snake robots since it can automate their applications in environments where human presence is unsafe or unwanted. However, underactuation, non-minimum phase zero dynamics, and complex motion patterns make this a challenging task where many research challenges still remain. In this paper, we show how sliding mode control techniques can be used to solve this problem. Our main motivation for using this technique for motion control of snake robots is the fact that these robots move on different surfaces with different friction properties. Accordingly, the necessity of developing control methods for snake robots which are robust w.r.t. changes in the environment of the robot is well-justified.

Path following control of snake robots has been considered in several previous works. The majority of these works consider snake robots with passive wheels, which is inspired by the world's first snake robot developed in 1972 [1], and which introduce sideslip constraints (i.e. nonholonomic velocity constraints) on the links of the robot. These constraints allow the control input to be specified directly in terms of the desired propulsion of the snake robot, which is employed in e.g. [2-5] for computed torque control of the position and heading of wheeled snake robots. Path following control of wheel-less (i.e. without velocity constraints) snake robots is only considered in a few previous works. In [6], path following control of swimming snake robots is achieved by moving the joints according to a predetermined gait pattern while introducing an angular offset in each joint to steer the robot to some desired path. Methods based on numerical optimal control are considered in [7] for determining optimal gaits during positional control of snake robots. In [8,9] cascaded systems theory is employed to achieve path following control of a snake robot described by a simplified model. Sliding mode control of the joint angles of a snake robot is considered in [10]. This work does, however, not consider the underactuated DOF of the robot.

The first contribution of this paper is to derive a partially feedback linearized Poincaré representation of the equations of motion of a snake robot without velocity constraints, which gives a detailed mathematical description of the system behaviour that can be used for analysis and model-based control design. To our best knowledge, the only previous work which derives the dynamic model of unconstrained (i.e. without velocity constraints) snake robots in a geometric mechanics framework is [11]. However, that work employs general affine differential geometry in contrast with the particular Poincaré representation in the present work. Furthermore, we add parametric modelling uncertainties due to changes in the friction coefficients to this model. We also

Ehsan Rezapour, Kristin Y. Pettersen, and Jan T. Gravdahl are with the Department of Engineering Cybernetics, Norwegian University of Science and Technology, NO-7491 Trondheim, Norway. emails: {ehsan.rezapour, kristin.y.pettersen, jan.tommy.gravdahl}@itk.ntnu.no. The affiliation of Pål Liljebäck is shared between the Department of Engineering Cybernetics and the Department of Applied Cybernetics, SINTEF ICT, NO-7465 Trondheim, Norway. email: {pal.liljebaeck@sintef.no}. This work was partly supported by the Research Council of Norway through project no. 205622 and its Centres of Excellence funding scheme, project no. 223254.

present a partial feedback linearization of the resulting model that makes it more suitable for model-based control design. The second contribution of this paper is development of a robust guidance-based path following control approach for snake robots. Guidance-based control strategies are common in e.g. marine control systems (see e.g. [12]). These control strategies are based on defining a desired heading angle for the vehicle through a guidance law, and subsequently designing a controller to track this angle. To our best knowledge, the only previous works which present formal stability proofs for guidance-based path following control of unconstrained snake robots are presented in [9] and [17]. The control design in [9] is, however, based on a simplified model of the robot, which is only valid for small joint angles. These simplifying assumptions are not present in the model considered in this paper. In contrast with [17], we use a similar idea for the orientation control design, but we use sliding mode techniques which make the design robust w.r.t. the modelling uncertainties, and we present formal stability proofs for the robust guidance-based control of a wheel-less snake robot.

The paper is organized as follows. In Section II, we develop a model of the snake robot dynamics in a differential geometry setting. In Section III, we state the control design objectives. In Section IV and V, we use sliding mode techniques to develop tracking controllers for the joints and the head angle of the robot, respectively. Finally, Section VI presents the simulation results which validate the theoretical results.

II. MODELLING

A. Geometry and Kinematics of the Snake Robot

A planar N-link snake robot evolves naturally in the configuration space $\mathcal{Q} = \mathcal{S} \times \mathcal{G}$, which is composed of a shape space $\mathcal{S}$ and a Lie group $\mathcal{G}$. In particular, the set of variables that define the internal configuration of the robot take values in $\mathcal{S}$. These are the relative joint angles of the robot which are equipped with DC motors as actuators, and which in coordinates we denote by $q_a = (\phi_1, \phi_2, ..., \phi_{N-1}) \in \mathcal{S}$. Moreover, the position variables which define the orientation and the position of the robot in the plane, lie in $\mathcal{G}$. These are passive DOF of the system which in coordinates we denote by $q_u = (\theta_N, p_x, p_y) \in \mathcal{G}$. The map between the absolute i-th link angle and (q_a, θ_N) is given by $\theta_i = \sum_{n=i}^{N-1} \phi_n + \theta_N$. The links of the robot are assumed to have uniformly distributed mass and moment of inertia. Thus, the planar position of the CM of the robot is defined as the average of the position of the CM of the individual links as

$$(p_x, p_y) = (\frac{1}{N}\sum_{i=1}^{N} x_i, \frac{1}{N}\sum_{i=1}^{N} y_i) \tag{1}$$

Consequently, the total configuration vector of the system is

$$q = [\phi_1, \phi_2, ..., \phi_{N-1}, \theta_N, p_x, p_y]^T \in \mathcal{Q} \tag{2}$$

The velocity space of the system is the $(2N+4)$-dimensional tangent bundle of the configuration manifold which we denote by $T\mathcal{Q}$. Since in this paper we consider a snake robot without velocity constraints, the velocity vector of the system has equal dimension to the configuration vector and is given by the time-derivative of (2) as

$$v = [\dot{\phi}_1, \dot{\phi}_2, ..., \dot{\phi}_{N-1}, \dot{\theta}_N, \dot{p}_x, \dot{p}_y]^T \in T\mathcal{Q} \tag{3}$$

So far we have defined all the kinematic parameters that we need for the control design. For a complete derivation of the kinematic map for the snake robot see e.g. [8].

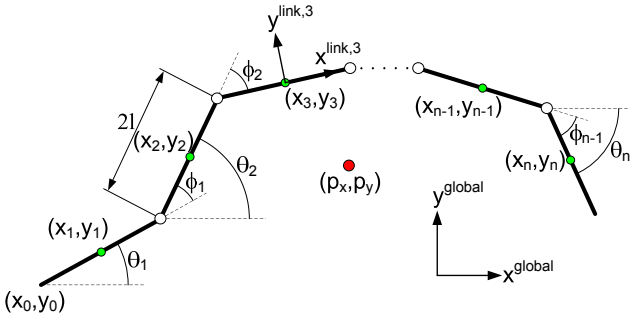

Fig. 1: Kinematic parameters of the snake robot

B. Equations of Motion

In this sub-section, we derive the Poincaré representation of the equations of motion of the snake robot. The majority of the previous works on snake robots have derived these equations based on a Newton-Euler formulation. However, we believe that formulating the equations of motion of the system in a geometric mechanics setting can be particularly useful for effectively addressing problems regarding the fundamental properties of snake robot motion. In particular, it is interesting both for controllability analysis and motion planning algorithms which are derived based on differential geometric approaches to mechanics, see e.g. [14].

Snake robots are a class of *simple* mechanical control systems, where the Lagrangian function $\mathcal{L} : T\mathcal{Q} \to \mathbb{R}$ is defined as the difference between the kinetic energy w.r.t. a Riemannian metric and the potential energy of the system. For geometric modelling of the system, we first write the kinetic energy of the i-th link as the sum of the translational and rotational kinetic energy of the link

$$\mathcal{K}_i(q, v) = \frac{1}{2} m(\dot{x}_i^2 + \dot{y}_i^2) + \frac{1}{2} J \dot{\theta}_i^2 \tag{4}$$

where m and J denote the mass and moment of inertia of the link, respectively. Thus, the total kinetic energy for the N-link robot is defined as the sum of the kinetic energy of the individual links as

$$\mathcal{K}(q, v) = \sum_{i=1}^{N} \mathcal{K}_i(q, v) \tag{5}$$

The kinetic energy of the snake robot defines a Riemannian metric on the configuration space that can be written as

$$\mathbb{G}_{ij}(q) = \frac{\partial^2 \mathcal{K}(q, v)}{\partial v^i \partial v^j} \tag{6}$$

where $\mathbb{G}_{ij}$ denotes the (i, j) component of the positive defi-

nite matrix-valued function $\mathbb{G}$. One can derive the Christoffel symbols of the second kind (see e.g. [14]) associated with the Riemannian metric of the robot in the form

$$\Gamma^k_{ij}(q) = \frac{1}{2}\mathbb{G}^{kl}(\frac{\partial \mathbb{G}_{il}}{\partial q^j} + \frac{\partial \mathbb{G}_{jl}}{\partial q^i} - \frac{\partial \mathbb{G}_{ij}}{\partial q^l}) \tag{7}$$

where i,j,k,$l \in \{1, ..., N+2\}$, and $\mathbb{G}^{kl}$ denotes the (k,l) component of $\mathbb{G}^{-1}$. Note that the summation convention is applied in (7), and henceforth, to all the repeated superscript and subscript indices (i.e. whenever an expression contains a repeated index, one as a subscript and the other as a superscript, summation is implied over this index [14]). Using the Riemannian metric and the Christoffel symbols, it is possible to derive the equations of motion of the system on the configuration space w.r.t. (q, v) as

$$\dot{q}^i = v^i \tag{8}$$

$$\dot{v}^i = -\Gamma^i_{jk} v^j v^k - \mathbb{G}^{ik} F^{\text{diss}}_k + \sum_{a=1}^{N-1} \mathbb{G}^{ik} F^a_k u^a \tag{9}$$

where $u = [u^1, ..., u^{N-1}] \in \mathbb{R}^{N-1}$ denotes the vector of control inputs which take values in the control set $U = \mathbb{R}^{N-1}$. Moreover, $F^{\text{diss}}_k \in T^*\mathcal{Q}$ denotes the external forces due to ground friction which take values in the cotangent bundle $T^*\mathcal{Q}$ (see e.g. [14]). Furthermore, $F = \{F^1, F^2, \ldots, F^{N-1}\} = \{d\phi_1, d\phi_2, ..., d\phi_{N-1}\}$ is the collection of the input covector fields of the system on $\mathcal{Q}$. Since the codistribution generated by the $N-1$ input covector fields cannot span $T^*\mathcal{Q}$, the snake robot is underactuated at any point of the configuration space. This underactuation reflects the fact that the input forces cannot set accelerations instantaneously in all directions of $\mathcal{Q}$ [15], i.e. the directions of the underactuated configuration variables. Note that since the robot moves in the horizontal plane orthogonal to the direction of the gravitational field, there exists no gravitational term in the system dynamics (8-9). The above Poincaré representation is called the *natural representation*, and it has the property that the equations may also be written in the following second-order form [14]

$$\ddot{q}^i + \Gamma^i_{jk}\dot{q}^j\dot{q}^k + \mathbb{G}^{ik}F^{\text{diss}}_k = \sum_{a=1}^{N-1} \mathbb{G}^{ik}F^a_k u^a \tag{10}$$

where $\ddot{q}^i = \dot{v}^i$. We have already specified all the elements of (10) except F^{diss}, which is the subject of the next subsection.

C. The Ground Friction Model

In this sub-section, a viscous friction model is used for capturing the essential properties of the anisotropic ground friction forces acting on the system during motion on *flat surfaces*. For modelling the friction, we first define the rotation matrix for mapping from the global coordinate frame to the local coordinate frame of link i, cf. Fig. 1, as

$$R_i = \begin{bmatrix} \cos\theta_i & -\sin\theta_i \\ \sin\theta_i & \cos\theta_i \end{bmatrix} \tag{11}$$

Using (11), the velocity of the i-th link in the local coordinate frame of the link can be written in terms of the velocity of the i-th link in the global coordinate frame, i.e. $(\dot{x}_i, \dot{y}_i)$, as

$$v^{\text{link},i} = \begin{bmatrix} v^{\text{link},i}_t \\ v^{\text{link},i}_n \end{bmatrix} = R_i^T \begin{bmatrix} \dot{x}_i \\ \dot{y}_i \end{bmatrix} \tag{12}$$

where $v^{\text{link},i}_n$ and $v^{\text{link},i}_t$ denote the linear velocity of the i-th link in the normal and tangential direction of the link, respectively. Assuming equal friction coefficients for all the links, the friction force acting on link i is defined as

$$f^{\text{link},i} = \begin{bmatrix} c_t v^{\text{link},i}_t & c_n v^{\text{link},i}_n \end{bmatrix}^T \tag{13}$$

where c_t and c_n denote the viscous friction coefficients in the tangential and normal direction of the link, respectively. Subsequently, we map the friction force acting on each link to the global coordinate frame as

$$f^{\text{link},i}_{\text{global}} = R_i f^{\text{link},i} \tag{14}$$

Finally, we can write F^{diss} in (10) as

$$F^{\text{diss}} = \sum_{i=1}^{N} \mathcal{J}_i^T(q) f^{\text{link},i}_{\text{global}} \tag{15}$$

where

$$\mathcal{J}_i^T(q) = \left[\frac{\partial \dot{x}_i}{\partial v_j}, \frac{\partial \dot{y}_i}{\partial v_j}\right] \in \mathbb{R}^{(N+2)\times 2}, j \in \{1, ..., N+2\} \tag{16}$$

denotes the transpose of the Jacobian matrix of the CM of the i-th link.

D. Partial Feedback Linearization of the Geometric Model

For performing a model-based control design, we would like to write the model in the simplest possible form. Feedback linearization is a common technique that can simplify the model by cancellation of the nonlinear terms. However, due to the lack of direct independent control for some configuration variables of the system, this technique cannot be directly applied to the snake robot dynamics. Thus, in this case we use partial feedback linearization which linearizes the dynamics of the fully actuated configuration variables, i.e. dynamics of q_a. To this end, we separate the vector of the generalized coordinates q into two parts, in the form $q = [q_a, q_u]^T \in \mathbb{R}^{N+2}$, where $q_a \in \mathbb{R}^{N-1}$ and $q_u \in \mathbb{R}^3$ were defined in Section II.A. Note that for clarity of presentation of the control design, henceforth we consider a local parametrization of the configuration space in an open subset of the Euclidean space. A partially feedback linearized Newton-Euler formulated model of snake robots was presented in [8], and we here extend it to a geometric model of the robot that is subject to parametric modelling uncertainties. This new model can be used for model-based robust control design for snake robots.

The dynamic model (10) is not suitable for partial feedback linearization. This is due to the presence of more than one input force in every scalar subsystem of (10). We note that this is the consequence of multiplying F by $\mathbb{G}^{-1}$ in the

right-hand side of (10). To obtain a suitable form of (10) for partial feedback linearization, we change the Christoffel symbols of the second kind (7), with those of the first kind using the relation

$$\Gamma_{jkl} = \sum_{i=1}^{N+2} \mathbb{G}_{li}\Gamma^i_{jk} \tag{17}$$

This changes (10) to the following form which is previously derived in [11], where the model is called the *locomotion dynamics* of the snake robot given by

$$\sum_{j=1}^{N+2} \mathbb{G}_{kj}\ddot{q}^j + \sum_{i=1}^{N+2}\sum_{j=1}^{N+2} \Gamma_{ijk}\dot{q}^i\dot{q}^j = \tau_k - F_k^{\text{diss}} \tag{18}$$

where $\tau = Fu = [\psi_1, ...\psi_{N-1}, 0, 0, 0] \in \mathbb{R}^{N+2}$ denotes the vector of input torques, in which ψ_i denotes the control torque provided by the actuator in the i-th robot joint. The dynamic model (18) is consistent with the well-known second-order Lagrangian equations of motion in the sense that in the left-hand side the first term is an acceleration related inertia term, the second term represents the Coriolis and centrifugal forces, and the right-hand side terms stand for external forces due to the controls and friction [11]. The dynamic model (18) is suitable for the aim of partial feedback linearization, since it can be separated into actuated and underactuated dynamics:

$$\begin{aligned} \sum_{j=1}^{N-1} \mathbb{G}_{mj}(q_a)\ddot{q}_a^j + \sum_{p=N}^{N+2} \mathbb{G}_{mp}(q_a)\ddot{q}_u^p + h_m(q,\dot{q}) = \quad \psi_m \\ \sum_{j=1}^{N-1} \mathbb{G}_{kj}(q_a)\ddot{q}_a^j + \sum_{p=N}^{N+2} \mathbb{G}_{kp}(q_a)\ddot{q}_u^p + h_k(q,\dot{q}) = 0 \end{aligned} \tag{19}$$

where $m \in \{1, ..., N-1\}$, $k \in \{N, ..., N+2\}$, and $h(q, \dot{q})$ contain all the contributions of the Coriolis, centrifugal and friction forces in (18). Since the objective of this paper is to develop a path following controller that is robust w.r.t. model uncertainties resulting from different friction properties, we will furthermore extend the locomotion dynamics model of [11], by adding these uncertainties to the model. In order to add parametric modelling uncertainties due to changes in the friction coefficients, we divide the vector $h \in \mathbb{R}^{N+2}$ in accordance with $[q_a, q_u]^T \in \mathbb{R}^{N+2}$ into two parts as $h = [h_a, h_u]^T \in \mathbb{R}^{N+2}$, and present the following assumption.

A.I *The terms $h_a(q, \dot{q})$ and $h_u(q, \dot{q})$ are perturbed with multiplicative uncertainties in the form*

$$h_a = (I_1 + \Delta_1)\hat{h}_a \in \mathbb{R}^{N-1} \tag{20}$$

$$h_u = (I_2 + \Delta_2)\hat{h}_u \in \mathbb{R}^3 \tag{21}$$

where $\hat{h}_a$ and $\hat{h}_u$ are the estimations of the actual h_a and h_u, respectively. Moreover, $I_1 \in \mathbb{R}^{(N-1)\times(N-1)}$ and $I_2 \in \mathbb{R}^{3\times3}$ are identity matrices. Furthermore, $\Delta_1 \in \mathbb{R}^{(N-1)\times(N-1)}$ and $\Delta_2 \in \mathbb{R}^{3\times3}$, are measures of parametric modelling uncertainties due to varying friction properties on surfaces.

For partial feedback linearization, we divide the matrix representation of the Riemannian metric as

$$\mathbb{G} = \begin{bmatrix} \mathbb{G}_{aa} & \mathbb{G}_{ua} \\ \mathbb{G}_{au} & \mathbb{G}_{uu} \end{bmatrix} \in \mathbb{R}^{(N+2)\times(N+2)} \tag{22}$$

where $\mathbb{G}_{aa} \in \mathbb{R}^{(N-1)\times(N-1)}$, $\mathbb{G}_{au} \in \mathbb{R}^{(N-1)\times3}$, $\mathbb{G}_{ua} \in \mathbb{R}^{3\times(N-1)}$, and $\mathbb{G}_{uu} \in \mathbb{R}^{3\times3}$ denote the corresponding submatrices. We may now write (19) in the matrix form:

$$\mathbb{G}_{aa}(q_a)\ddot{q}_a + \mathbb{G}_{au}(q_a)\ddot{q}_u + h_a(q,\dot{q}) = \psi \in \mathbb{R}^{N-1} \tag{23a}$$

$$\mathbb{G}_{ua}(q_a)\ddot{q}_a + \mathbb{G}_{uu}(q_a)\ddot{q}_u + h_u(q,\dot{q}) = 0_{3\times1} \in \mathbb{R}^3 \tag{23b}$$

where $\psi = [\psi_1, ...\psi_{N-1}]^T \in \mathbb{R}^{N-1}$, and $0_{3\times1}$ denotes the column vector of zeros with dimension 3. From (23b) we have

$$\ddot{q}_u = -\mathbb{G}_{uu}^{-1}(\mathbb{G}_{ua}\ddot{q}_a + (I_2 + \Delta_2)\hat{h}_u) \tag{24}$$

Inserting (24) into (23a) yields

$$(\mathbb{G}_{aa} - \mathbb{G}_{au}\mathbb{G}_{uu}^{-1}\mathbb{G}_{ua})\ddot{q}_a = \psi + \mathbb{G}_{au}\mathbb{G}_{uu}^{-1}(I_2+\Delta_2)\hat{h}_u - (I_1+\Delta_1)\hat{h}_a \tag{25}$$

To cancel out the nonlinear terms in the actuated subset of the equations of motion, we define the control inputs as

$$\psi = (\mathbb{G}_{aa} - \mathbb{G}_{au}\mathbb{G}_{uu}^{-1}\mathbb{G}_{ua})\vartheta - \mathbb{G}_{au}\mathbb{G}_{uu}^{-1}\hat{h}_u + \hat{h}_a \tag{26}$$

where $\vartheta = [\vartheta_1, \vartheta_2, ..., \vartheta_{N-1}]^T \in \mathbb{R}^{N-1}$ is the new vector of control inputs. Finally, by inserting (26) into (25), we obtain the dynamics of the system in a control-affine with drift form

$$\begin{aligned} \ddot{q}_a &= \vartheta + G_a(q,\dot{q}) \in \mathbb{R}^{N-1} \\ \ddot{q}_u &= f(q,\dot{q}) + G_u(q,\dot{q}) + g(q_a)\vartheta \in \mathbb{R}^3 \end{aligned} \tag{27}$$

with

$$\begin{aligned} f &= -\mathbb{G}_{uu}^{-1}\hat{h}_u = [f_{\theta_N}, f_x, f_y]^T \in \mathbb{R}^3 \\ g_i &= -\mathbb{G}_{uu}^{-1}\mathbb{G}_{ua} = [\beta_i, 0, 0]^T \in \mathbb{R}^3 \\ G_a &= \Delta_1\hat{h}_1 - \mathbb{G}_{au}\mathbb{G}_{uu}^{-1}\Delta_2\hat{h}_u = [G_1, ..., G_{N-1}]^T \in \mathbb{R}^{N-1} \\ G_u &= -\mathbb{G}_{uu}^{-1}\Delta_2\hat{h}_u = [G_{\theta_N}, G_x, G_y]^T \in \mathbb{R}^3 \end{aligned}$$

where g_i denotes the i-th column of $g \in \mathbb{R}^{3\times(N-1)}$ in which $\beta_i(q_a) : \mathbb{R}^{N-1} \to \mathbb{R}^{<0}$ is a smooth function.

A.II *We assume that $\beta_i(q_a)$ is negative-valued for all $i \in \{1, ..., N-1\}$ in any configuration of the robot.*

Remark I. *Both through numerical simulations and experiments, it can be verified that $\beta_i(q_a)$ is negative-valued for all $i \in \{1, ..., N-1\}$ in any configuration of the robot. This probably follows from the uniform positive-definiteness of the Riemannian metric of the robot.*

Moreover, in dynamic model (27), f_{θ_N}, f_x, and f_y denote the friction forces acting on θ_N, p_x, and p_y, respectively. (f_{θ_N} also contains Coriolis and centrifugal forces besides the friction forces). Furthermore, G_a and G_u denote the parametric modelling uncertainties in the dynamics of the fully actuated internal configuration variables and the dynamics of the underactuated position variables of the robot, respectively. In particular, the uncertain terms are upper bounded by some known positive-valued vector function $\varrho(q,\dot{q}) = [\varrho_1(q,\dot{q}), \varrho_2(q,\dot{q}), ..., \varrho_{N+2}(q,\dot{q})]^T \in \mathbb{R}^{N+2}_{>0}$, i.e. $\|G_i(q,\dot{q})\| \leq \varrho_i(q,\dot{q})$ for every $i \in \{1, ..., N+2\}$.

The partially feedback linearized model (27) is suitable for analysis and control design for snake robot. For the aim model-based control design, we write (27) in a detailed form

$$\ddot{q}_a = \vartheta + G_a(q,\dot{q}) \in \mathbb{R}^{N-1} \quad (28)$$

$$\ddot{\theta}_N = f_{\theta_N}(q,\dot{q}) + \beta_i(q_a)\vartheta^i + G_{\theta_N}(q,\dot{q}) \in \mathbb{R} \quad (29)$$

$$\ddot{p}_x = f_x(q,\dot{q}) + G_x(q,\dot{q}) \in \mathbb{R} \quad (30)$$

$$\ddot{p}_y = f_y(q,\dot{q}) + G_y(q,\dot{q}) \in \mathbb{R} \quad (31)$$

where $i \in \{1,...,N-1\}$.

III. CONTROL DESIGN OBJECTIVES

In this section, we state the control objectives for the controllers proposed in the subsequent sections. We first define a controlled output vector for the system in the form

$$Y = [\tilde{\phi}_1, \tilde{\phi}_2, ..., \tilde{\phi}_{N-1}, \tilde{\theta}, \tilde{p}_x, \tilde{p}_y]^T \in \mathbb{R}^{N+2} \quad (32)$$

Every element of Y denotes the error of the corresponding configuration variable w.r.t. its reference signal. Furthermore, we define three control objectives. The first part of the control objective is to make the internal configuration variables q_a (i.e. the body shape of the snake robot) asymptotically track time-varying references which will be defined in the next section. This control objective is defined as

$$\lim_{t\to+\infty} \|\tilde{\phi}_i(t)\| = 0 \quad (33)$$

for every $i \in \{1,...,N-1\}$.

The second control objective is to make the head angle of the robot, which is an underactuated DOF, track a reference head angle such that

$$\lim_{t\to+\infty} \|\tilde{\theta}(t)\| = 0 \quad (34)$$

The third control objective concerns the position of the snake robot w.r.t. a desired straight path. In particular, we define the desired path as a smooth one-dimensional manifold $\mathcal{P} \subset \mathbb{R}^2$, with coordinates in the $x-y$ plane given by the pair (p_{xd}, p_{yd}). These coordinates are parametrized by a time-dependent variable $\Theta(t) \in \mathbb{R}$ that is

$$\mathcal{P} = \{(p_{xd}(\Theta), p_{yd}(\Theta)) \in \mathbb{R}^2 : \Theta \geq 0\} \quad (35)$$

We define the control objective for the position of the CM of the robot as practical convergence to the desired path such that for the vector of the path following error variables $\tilde{p} = [p_{xd}(\Theta(t)) - p_x(t), p_{yd}(\Theta(t)) - p_y(t)]^T \in \mathbb{R}^2$ we have

$$\lim_{t\to+\infty} \sup \|\tilde{p}(t)\| \leq \bar{\varepsilon} \quad (36)$$

where $\bar{\varepsilon} \in \mathbb{R}^+$ is a positive constant that can be made arbitrarily small. Moreover, we require that $\dot{\Theta}(t) \geq 0$ and $\lim_{t\to\infty} \Theta(t) = \infty$ (i.e. that the snake robot moves forward along the path), and boundedness of the states of the system.

IV. SLIDING MODE TRACKING CONTROL OF THE JOINT ANGLES

In this section, we solve the control objective in (33) by defining the reference trajectories for the joints of the snake robot (i.e. the gait pattern), and by using sliding mode techniques to design a robust joint angle tracking control law.

It has previously been shown in [1] that the gait pattern lateral undulation, which is the most common type of snake locomotion, is achieved by moving the joints according to the *serpenoid curve*. The resulting reference joint angle trajectories are

$$\phi_{\mathrm{ref},i}(t) = \alpha \sin(\omega t + (i-1)\delta) + \phi_o \quad (37)$$

where α denotes the amplitude of the sinusoidal joint motion, ω denotes the angular frequency, δ is a phase shift that keeps the joints out of phase, and ϕ_o is an offset value that is identical for all the joints. Moreover, motivated by [8], where it is shown how ϕ_o can be used to steer the heading angle of the robot, we use the second-order time-derivative of ϕ_o as an additional guidance control term for the underactuated dynamics of the robot.

The powerful feature of sliding mode control is its robustness w.r.t. model uncertainties. For snake robots, this robustness is useful for performing robust control tasks on surfaces with varying friction properties. To design a robust tracking controller for the joints of the robot, we first define the vector of the reference joint trajectories as

$$q_{\mathrm{ref}}(t) = [\phi_{\mathrm{ref},1}, \phi_{\mathrm{ref},2}, ..., \phi_{\mathrm{ref},N-1}]^T \in \mathbb{R}^{N-1} \quad (38)$$

Thus, the vector of joint angle tracking errors is defined as

$$\Phi(t) = [\tilde{\phi}_1, \tilde{\phi}_2, ..., \tilde{\phi}_{N-1}]^T \in \mathbb{R}^{N-1} \quad (39)$$

where $\tilde{\phi}_i = \phi_{\mathrm{ref},i} - \phi_i$ denotes the i-th joint angle tracking error variable. We define the sliding mode variable for the joint angles of the robot as

$$s = \dot{\Phi} + K\Phi \in \mathbb{R}^{N-1} \quad (40)$$

where $K = \mathrm{diag}\{k_i\}_{i=1}^{N-1} \in \mathbb{R}^{(N-1)\times(N-1)}$ is a diagonal matrix of positive constant gains. The time-derivative of the sliding mode variable (40) is given by

$$\dot{s} = \ddot{\Phi} + K\dot{\Phi} \in \mathbb{R}^{N-1} \quad (41)$$

The control objective in (33) is achieved by stabilizing the sliding manifold $s = 0_{N-1}$ in finite time, and remaining on the manifold for all future time. To this end, we select a Lyapunov function candidate for (41) as

$$V = \frac{1}{2} s^T s \quad (42)$$

Taking the time-derivative of V along the solutions of (41) gives

$$\begin{aligned} \dot{V} &= s^T\dot{s} = s^T(\ddot{\Phi} + K\dot{\Phi}) = s^T(\ddot{q}_{\mathrm{ref}} - \ddot{q}_a + K\dot{\Phi}) \\ &= s^T(\ddot{q}_{\mathrm{ref}} - [\vartheta + G_a(q,\dot{q})] + K\dot{\Phi}) \end{aligned} \quad (43)$$

The typical structure of a robust controller is composed of a nominal part similar to a feedback linearizing or inverse control law, and of an additional term aimed at dealing with model uncertainty [16]. Consequently, we take the joint angle tracking control law as

$$\vartheta = \vartheta_{\mathrm{nom}} + \vartheta_{\mathrm{add}} \quad (44)$$

where

$$\vartheta_{\text{nom}} = (\ddot{q}_{\text{ref}} + K\dot{\Phi}) \in \mathbb{R}^{N-1} \quad (45)$$

$$\vartheta_{\text{add}} = \gamma \operatorname{sgn}(s) \in \mathbb{R}^{N-1} \quad (46)$$

and where $\gamma = \operatorname{diag}\{\gamma_i\}_{i=1}^{N-1} \in \mathbb{R}^{(N-1)\times(N-1)}$ is a diagonal matrix of positive constants. Moreover, we define $\operatorname{sgn}(s) = [\operatorname{sgn}(s_1), ..., \operatorname{sgn}(s_{N-1})]^T \in \mathbb{R}^{N-1}$. Substituting (44) into (43) yields

$$\dot{V} = s^T \left[-\gamma \operatorname{sgn}(s) - G_a(q, \dot{q})\right] \quad (47)$$

We take $\gamma_i = \gamma_0 + \varrho_i(q, \dot{q})$, where $\gamma_0 > 0$ is a constant. We note that the i-th term of $\dot{V}$ denoted by $\dot{V}_i$ is of the form

$$\begin{aligned}\dot{V}_i =& s_i(-\gamma_i \operatorname{sgn}(s_i) - G_i(q, \dot{q})) \leq \\ & -(\gamma_0 + \varrho_i(q, \dot{q}))s_i \operatorname{sgn}(s_i) + |s_i|\varrho_i(q, \dot{q}) \leq -\gamma_0|s_i|\end{aligned} \quad (48)$$

Consequently, $\dot{V} = -\sum_{i=1}^{N-1} \gamma_0|s_i|$ is negative-definite. This implies that the sliding manifold $s = 0_{N-1}$ is a positively invariant set for (41). The positive invariance property of $s = 0_{N-1}$ implies that once the solutions of (41) reach the sliding manifold, they cannot leave it and the motion of the joints will be restricted to this manifold. To show that the solutions of (41) reach the sliding manifold in finite time we use the *Comparison Lemma* (see e.g. [13]). In particular, we take $W = \sum_{i=1}^{N-1} \sqrt{2V_i} = \sum_{i=1}^{N-1} |s_i|$. The upper right derivative $D^+W = \sum_{i=1}^{N-1} \dot{V}_i \frac{1}{\sqrt{2V_i}}$ satisfies the differential inequality

$$D^+W \leq -(N-1)\gamma_0 \quad (49)$$

Using the comparison lemma we have that $W(s(t)) \leq W(s(0)) - (N-1)\gamma_0$, which implies that $W = \sum_{i=1}^{N-1} \sqrt{2V_i} = 0$ must reach $V_i = 0$ in finite time. Accordingly, the solutions of (41) starting off the positively invariant manifold $s = 0_{N-1}$ will reach it in finite time.

We summarize the results of the foregoing arguments in the following theorem.

Theorem I. *With the robust joint tracking control law (44), the solutions of (41) reach the sliding manifold $s = 0_{N-1}$ in finite time. The positive invariance of this manifold, which is shown by (48), implies that these solutions will remain on the sliding manifold for all future time. Moreover, exponential stability of the origin of the joint tracking error dynamics $\dot{\Phi} = -K\Phi$ on the sliding manifold, implies that the joint tracking errors exponentially converge to zero during the sliding phase, see [13], and the control objective (33) will be achieved.*

Remark II. *The discontinuous* $\operatorname{sgn}()$ *function in the sliding mode controller may lead to issues related to existence and uniqueness of solutions, issues related to the validity of the Lyapunov analysis, and chattering (see [13]). To avoid these issues, a common approach is to approximate the (discontinuous)* $\operatorname{sgn}(s)$ *function with a high slope (continuous) saturation function* $\operatorname{sat}(s/\varepsilon)$*. However, with this approximation the best we can achieve is ultimate boundedness of the tracking errors with an ultimate bound that can be controlled by the design parameter ε [13]. Also note that in the case that the snake robot parametric modelling uncertainties are non-vanishing in the origin $(\Phi, \dot{\Phi}) = (0_{N-1}, 0_{N-1})$, then the origin is not an equilibrium point that can be made asymptotically stable.*

V. UNDERACTUATED TRACKING CONTROL VIA SLIDING MODE DESIGN

In this section, we design a head angle controller for the snake robot in order to achieve the second controller objective (34). In particular, we analytically show that robust tracking control of the head angle of the robot can be achieved by using ϕ_o as an additional control term for the underactuated head angle of the robot. To this end, we use $\ddot{\phi}_o$ as a dynamic compensator which adds a similar extra offset angle to the sinusoidal parts of the reference joint trajectories such that the overall structure the robot converges to the desired path. Furthermore, we use sliding mode techniques to design the dynamic compensator in a way that this convergence will be achieved even in the presence of parametric modelling uncertainties due to friction changes.

A. Sliding Mode Control of the Head Angle

With the gait pattern lateral undulation (37), the reference joint trajectories are composed of non-identical sinusoidal parts, and an identical offset. Let us denote $S_i = \alpha \sin(\omega t + (i-1)\delta)$. Thus, the reference trajectory of the i-th joint is

$$\phi_{\text{ref},i} = S_i + \phi_o \quad (50)$$

The head angle dynamics in closed-loop form can be obtained by substituting the joint control law (44) into the head angle dynamics (29), which gives (arguments are excluded for notational convenience)

$$\begin{aligned}\ddot{\theta}_N =& f_{\theta_N} + G_{\theta_N} + \sum_{i=1}^{N-1} \beta_i \vartheta_i = \\ & f_{\theta_N} + G_{\theta_N} + \sum_{i=1}^{N-1} \beta_i(\ddot{S}_i + k_i\dot{S}_i - k_i\dot{q}_i) + \\ & \sum_{i=1}^{N-1} \beta_i(\ddot{\phi}_o + k_i\dot{\phi}_o + \gamma_i \operatorname{sgn}(s_i) + G_i)\end{aligned} \quad (51)$$

where G_i denotes the i-th component of the vector-valued function $G_a(q, \dot{q}) \in \mathbb{R}^{N-1}$. The goal of the control design is to make the head angle exponentially converge to a reference head angle. In the following, we show that this convergence can be achieved by using the additional control term $\ddot{\phi}_o$. To this end, we first define the error variable for the head angle of the robot as $\tilde{\theta} = \theta_{\text{ref}} - \theta_N$, where θ_{ref} denotes the reference head angle of the robot which will be defined in Section V.B. Moreover, we define the sliding mode variable for the head angle in the form

$$s_\theta = \dot{\tilde{\theta}} + \Lambda\tilde{\theta} \quad (52)$$

where $\Lambda > 0$ is a constant gain. The time-derivative of the sliding mode variable (52) is given by

$$\dot{s}_\theta = \ddot{\tilde{\theta}} + \Lambda\dot{\tilde{\theta}} \quad (53)$$

To stabilize the constraint manifold $s_\theta = 0$, we select a Lyapunov function candidate for (53) as

$$V_\theta = \frac{1}{2} s_\theta^2 \tag{54}$$

The time-derivative of V_θ along the solutions of (53) gives

$$\dot{V}_\theta = s_\theta \dot{s}_\theta = s_\theta(\ddot{\tilde{\theta}} + \Lambda \dot{\tilde{\theta}}) = s_\theta(\ddot{\theta}_{\text{ref}} - \ddot{\theta}_N + \Lambda \dot{\tilde{\theta}}) \tag{55}$$

By inserting $\ddot{\theta}_N$ from (51) into (55), we obtain

$$\begin{aligned} \dot{V}_\theta =& s_\theta[\ddot{\theta}_{\text{ref}} - f_{\theta_N} - G_{\theta_N} - \sum_{i=1}^{N-1} \beta_i(\ddot{S}_i + k_i \dot{S}_i - k_i \dot{q}_i) \\ & - \sum_{i=1}^{N-1} \beta_i(\ddot{\phi}_o + k_i \dot{\phi}_o + \gamma_i \operatorname{sgn}(s_i) + G_i) + \Lambda \dot{\tilde{\theta}}] \end{aligned} \tag{56}$$

In order to stabilize the sliding manifold $s_\theta = 0$ we take

$$\begin{aligned} \ddot{\phi}_o = & \frac{1}{\sum_{i=1}^{N-1} \beta_i}(\ddot{\theta}_{\text{ref}} - f_{\theta_N} - \sum_{i=1}^{N-1} \beta_i[\ddot{S}_i + k_i \dot{S}_i - k_i \dot{q}_i \\ & + k_i \dot{\phi}_o + \gamma_i \operatorname{sgn}(s_i)] + \Lambda \dot{\tilde{\theta}} + \gamma_\theta \operatorname{sgn}(s_\theta)) \end{aligned} \tag{57}$$

where $\gamma_\theta > 0$ is a constant gain. Since β_i is a negative-valued function for all $i \in \{1, ..., N-1\}$, (57) is globally well-defined. In this work, through numerical simulations we show that the states of the dynamic compensator (57), i.e. $(\phi_o, \dot{\phi}_o)$, remain bounded, however, a formal proof of this boundedness will be presented elsewhere. We define $\gamma_\theta = \gamma_{\theta_0} + \varrho_N(q, \dot{q})$ for some $\gamma_{\theta_0} > 0$. Inserting (57) into (56) yields

$$\begin{aligned} \dot{V}_\theta = & s_\theta(-\gamma_\theta \operatorname{sgn}(s_\theta) - G_{\theta_N}) \leq \\ & - (\gamma_{\theta_0} + \varrho_N(q, \dot{q})) s_\theta \operatorname{sgn}(s_\theta) + |s_\theta| \varrho_N(q, \dot{q}) \leq -\gamma_{\theta_0} |s_\theta| \end{aligned} \tag{58}$$

The negative-definiteness of $\dot{V}_\theta$ implies the positive invariance of the sliding manifold $s_\theta = 0$ for (53). This implies that once solutions of (53) reach $s_\theta = 0$, they will remain there for all future time.

The results of the foregoing arguments is summarized in the following theorem.

Theorem II. *Inequality (58) along with the comparison lemma [13], imply that all solutions of (53) starting off the manifold $s_\theta = 0$, will reach it in finite time, and solutions on the manifold cannot leave it. Moreover, the exponential stability of the origin of the head angle error dynamics $\dot{\tilde{\theta}} = -\Lambda \tilde{\theta}$ on the sliding manifold, implies that during the sliding phase, the head angle error converges exponentially fast to zero, and the control design objective (34) will be achieved.*

B. The Path Following Guidance Law

In this sub-section, we target the third and last control objective in (36) by defining a Line-of-Sight (LOS) guidance law in order to make the position of the CM of the snake robot denoted by (p_x, p_y), converge to and follow a desired straight path. Without loss of generality, we assume that the desired path is always aligned with the global x-axis, i.e. $p_{yd} \equiv 0$. As a result, p_y denotes the Euclidean distance from the robot to the desired path, often referred to as the *cross-track error*. We choose the head angle reference according to the following LOS guidance law

$$\theta_{\text{ref}} = -\arctan(p_y / \Delta) \tag{59}$$

where $\Delta > 0$ is a constant parameter called the Look-Ahead-Distance. The idea is that steering the head angle of the snake robot such that it is headed towards a point located a distance Δ ahead of the robot along the desired path, will make the snake robot move towards the path and follow it.

We conjecture that the proposed guidance-based path following control strategy steers the position of the CM of the robot towards the desired path, and drives it along the path even in the presence of parametric modelling uncertainties. The next section presents simulation results which support this conjecture. However, a formal proof of this conjecture remains a topic of future work.

VI. SIMULATION RESULTS

In this section, the results of simulations of the path following controller based on the complete model that we developed throughout Section II are presented. We test our control approach on a snake robot with $N = 4$ links. However, these results are generalizable to snake robots with more number of links. The inertial parameters of the links were $m = 0.5$ kg, $l = 0.1$ m, and $J = 0.0016$ kgm^2. The parameters of the joint reference trajectory in (37) were $\alpha = \pi/6$ rad, $\omega = 80\pi/180$ rad/s, and $\delta = 2\pi/3$ rad. The sliding mode controller gains were $K = \text{diag}\{2\}_{i=1}^3$, $\gamma = \text{diag}\{15\}_{i=1}^3$, $\Lambda = 4$, and $\gamma_\theta = 10$. The look-ahead-distance was $\Delta = 3$ m. We considered the initial conditions $(q, \dot{q}) = (0_{N+1}, -5, 0_{N+2})$, i.e. all the initial conditions were set to zero, except 5 meters initial cross-track error.

To show the robustness of the proposed feedback law w.r.t. the modelling uncertainties due to friction forces, we assumed that the identified ground friction coefficients were $c_n = 10$, and $c_t = 1$, while the actual coefficients were $c_n = 20$, and $c_t = 2$. The simulation results show that the proposed control strategy successfully steers the snake robot towards the desired path and drives it along the path.

VII. CONCLUSIONS

In this paper we have considered the problem of robust path following control of wheel-less planar snake robots. We derived the equations of motion of the robot in a geometric mechanics setting. We used sliding mode techniques to design a robust tracking controller for the joint angles of the robot to track a desired gait pattern. Furthermore, we designed a dynamic compensator to control the head angle of the robot to a Line-of-Sight Guidance law. The simulation results verified the theoretical results and showed that the robot successfully converged to and followed the desired planar path in the presence of parametric modelling uncertainties. A formal proof of this convergence remains a topic of future work.

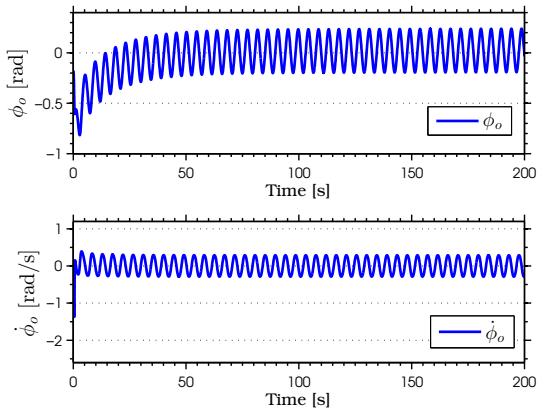

Fig. 2: The solutions of the dynamic compensator converge to a neighbourhood of the origin, after compensating for the head angle error

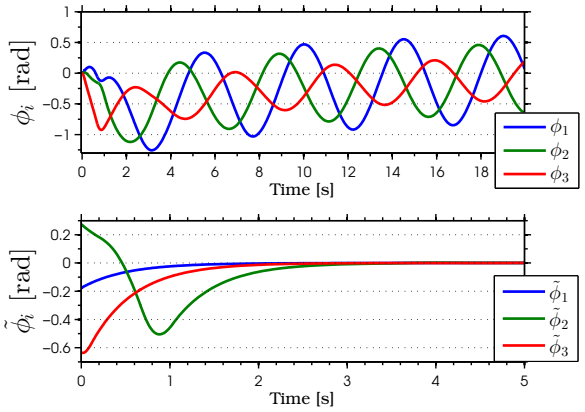

Fig. 3: The joints of the robot track the serpentine motions (above). The joint tracking errors converge to zero exponentially (below)

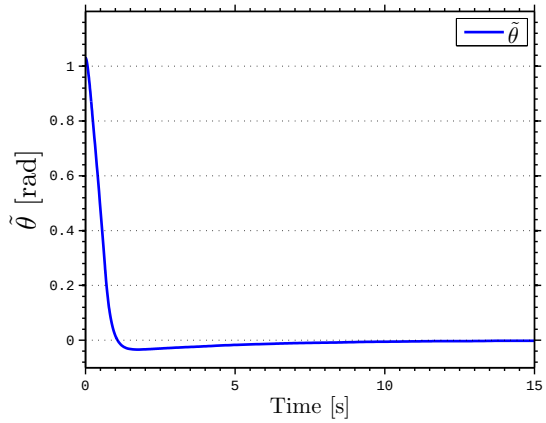

Fig. 4: The head angle tracking error converges to zero exponentially

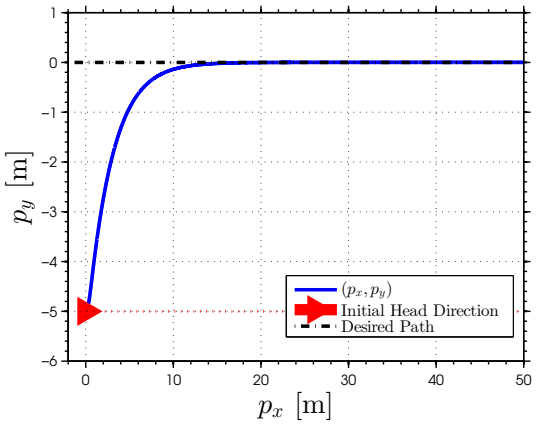

Fig. 5: The position of the CM of the robot (blue) follows the desired straight line path (the x-axis).

REFERENCES

[1] S. Hirose, "Biologically Inspired Robots: Snake-Like Locomotors and Manipulators", Oxford University Press, 1993.

[2] P. Prautsch, T. Mita, and T. Iwasaki, "Analysis and control of a gait of snake robot", *Transactions-Institute of Electrical Engineers of Japan*, D-120.3. pp. 372-381. 2000.

[3] H. Date, Y. Hoshi, and M. Sampei, "Locomotion control of a snake-like robot based on dynamic manipulability", in Proc. IEEE/RSJ Int. Conf. Intelligent Robots and Systems, Takamatsu, Japan, 2000.

[4] S. Ma, Y. Ohmameuda, K. Inoue, and B. Li, "Control of a 3-dimensional snake-like robot", in Proc. IEEE Int. Conf. Robotics and Automation, vol. 2, pp. 2067-2072, Taipei, Taiwan, 2003.

[5] M. Tanaka and F. Matsuno, "Control of 3-dimensional snake robots by using redundancy", in Proc. IEEE Int. Conf. Robotics and Automation, pp. 1156-1161, Pasadena, CA, 2008.

[6] K. McIsaac and J. Ostrowski, "Motion planning for anguilliform locomotion", *IEEE Transactions on Robotics and Automation*, vol. 19, no. 4, pp. 637-652, 2003.

[7] G. Hicks and K. Ito, "A method for determination of optimal gaits with application to a snake-like serial-link structure", *IEEE Transactions on Automatic Control*, vol. 50, no. 9, pp. 1291-1306, 2005.

[8] P. Liljebäck, K. Y. Pettersen, Ø. Stavdahl, and J. T. Gravdahl, "Snake Robots-Modelling, Mechatronics, and Control", Advances in Industrial Control. Springer, 2013.

[9] P. Liljebäck, I. U. Haugstuen, and K. Y. Pettersen, "Path following control of planar snake robots using a cascaded approach", *IEEE Transactions on Control Systems Technology*, no.20, 111-126, 2012.

[10] M. Haghshenas-Jaryani, G. Vossoughi, "Modeling and Sliding Mode Control of a Snake-Like Robot with Holonomic Constraints", in Proc. IEEE Int. Conf. on Robotics and Biomimetics, Bangkok, 2009.

[11] Z. Wang, S. Ma, B. Li, and Y. Wang, "A unified dynamic model for locomotion and manipulation of a snake-like robot based on differential geometry", *Science China Information Sciences*, 54, no. 2: 318-333, 2011.

[12] T. I. Fossen, "Marine control systems: Guidance, navigation and control of ships, rigs and underwater vehicles", Marine Cybernetics, Trondheim, Norway, 2002.

[13] H. K. Khalil, "Nonlinear Systems", Third ed., Englewood cliffs, NJ: Prentice-Hall, 2002.

[14] F. Bullo, A. Lewis, "Geometric Control of Mechanical Systems", Springer, 2005.

[15] H. Goldstein, "Classical Mechanics", 2nd ed. Reading, MA: AddisonWesley, 1980.

[16] J. J. Slotine and W. Li, "Applied nonlinear control", Prentice-Hall, NJ, 1991.

[17] E. Rezapour, K.Y. Pettersen, P. Liljebck and J.T. Gravdahl, "Path Following Control of Planar Snake Robots Using Virtual Holonomic Constraints", in Proc. 2013 IEEE Int. Conf. on Robotics and Biomimetics, Shenzhen, China, 12-14 Dec. 2013.